CEB

Steel Quality and Static Analysis

Rolf Eligehausen

Rolf Eligehausen, Prof. Dr.-Ing., Institute for Material Science in Civil Engineering
University of Stuttgart, Pfaffenwaldring 4, D-W 7000 Stuttgart 80

Eckhart Fabritius

Eckhart Fabritius, Dipl.-Ing., Institute for Material Science in Civil Engineering
University of Stuttgart, Pfaffenwaldring 4, D-W 7000 Stuttgart 80

Steel Quality and Static Analysis

by

R. Eligehausen and E. Fabritius
University of Stuttgart

1 Introduction

Reinforced concrete structures show a pronounced non-linear behavior with increasing load. This can be seen from Fig. 1, which gives the midspan deflection of a beam as a function of the applied load.

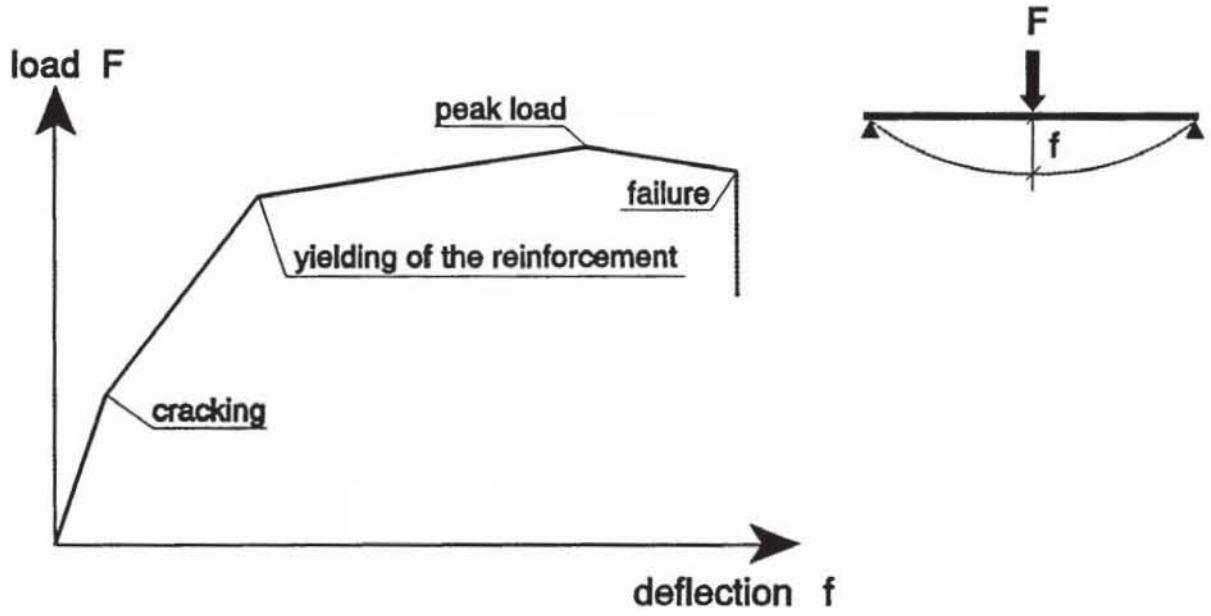

Figure 1: Typical load-deflection diagramm of a beam

Up to the cracking load the structure behaves linear elastically. Cracking decreases the stiffness significantly leading to larger deflections. At yielding of the reinforcement a plastic hinge is formed in the region of the maximum moment. While the increase in load up to the peak load is rather small, the increase in deflection may be rather large. The peak load is reached when either some bars of the reinforcement reach their tensile strength or the concrete in the most stressed fibre begins to crush.

In a deformation controlled test, the deflections can be increased further with decreasing beam resistance. Failure may be due to rupture of the reinforcement or crushing of the concrete. The length of the descending branch of the load-deflection curve is rather small in case of a steel failure and may be significant in case of a concrete failure.

Fig. 2 shows plastic hinges with bending cracks or shear cracks, respectively. Inclined shear cracks will occur if the shear stresses are sufficiently high.

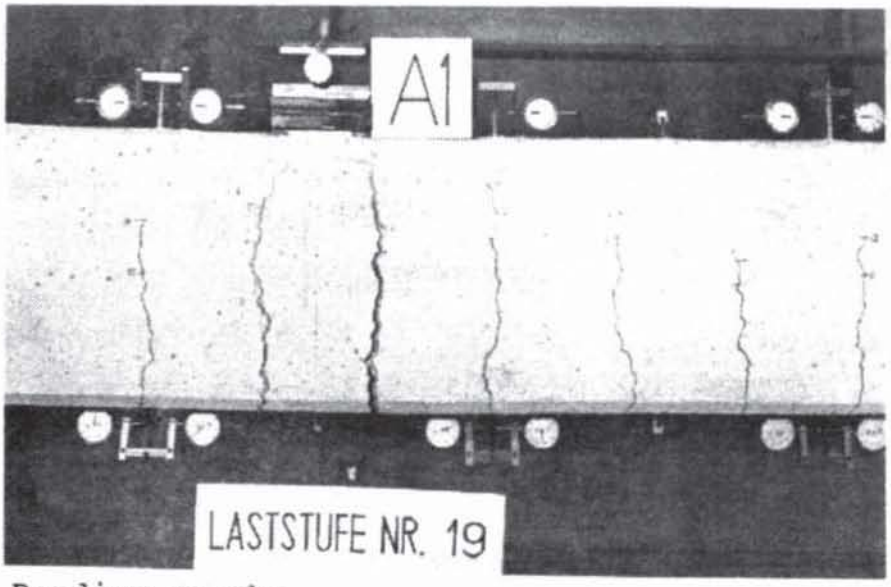

a.) Bending cracks

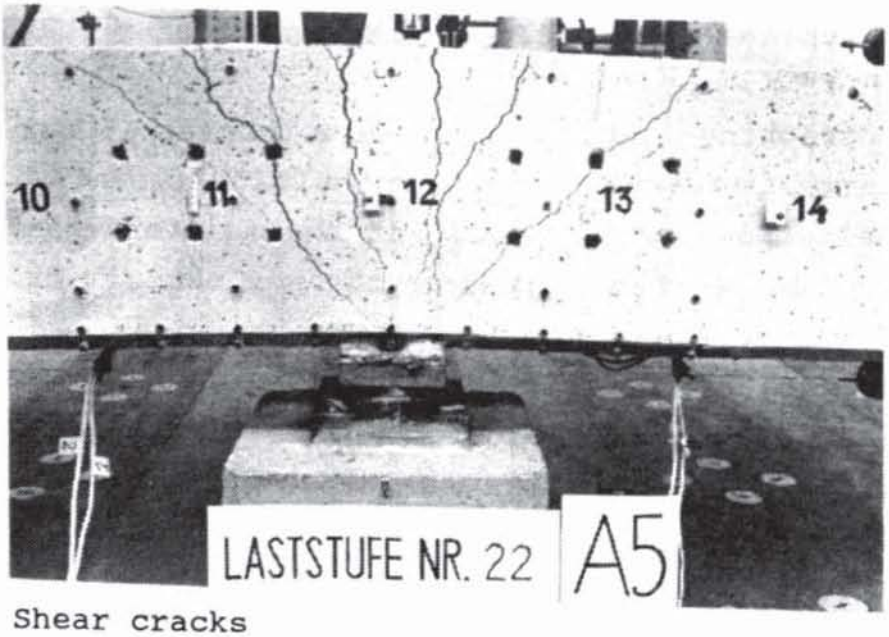

b.) Shear cracks

Figure 2: Plastic hinges (after Bachmann/Thürlimann (1965))

The non-linear behavior influences the distribution of internal forces in an indeterminate structure. This will be explained for the continuous beam under uniformly distributed loads shown in Fig. 3a. In Fig. 3b the beam deflections are plotted. Fig. 3c shows the moment distribution assuming elastic behavior of the beam with no (δ=1,0) and with 50 % (δ=0,5) moment redistribution of the elastic support moment.

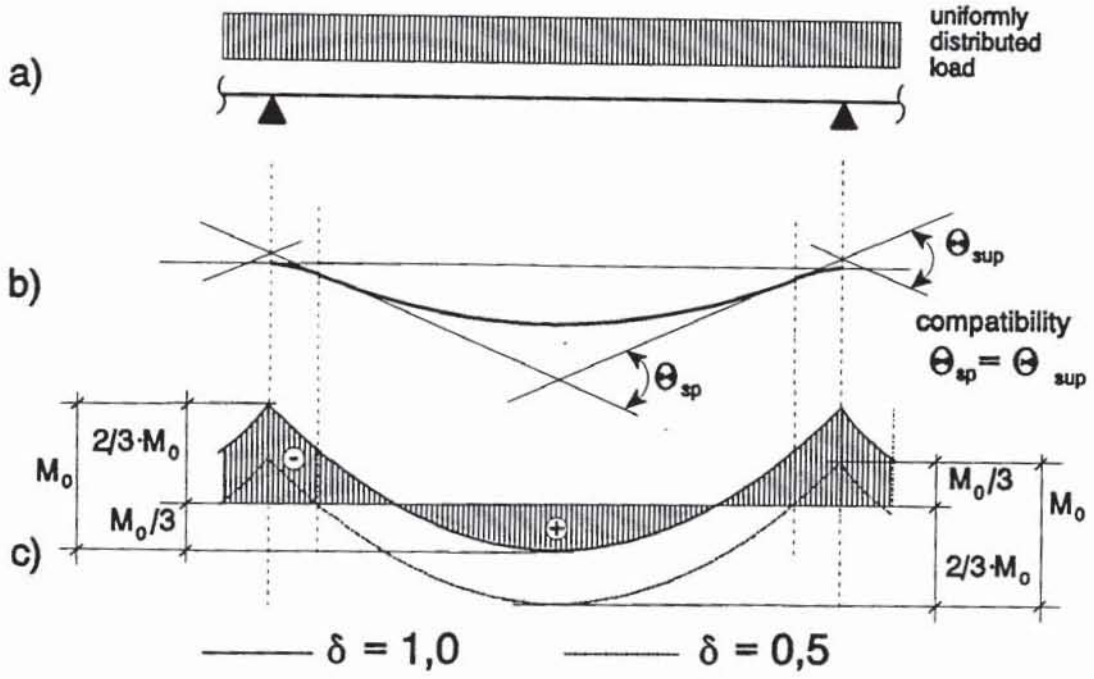

Figure 3: Continous beams under uniformly distributed loads

a) statical system
b) deflection curve
c) moment distribution for elastic behavior (δ=1,0) and 50% moment redistribution (δ=0,5)

In Fig. 4 the development of the moments in the span and over the support is plotted as a function of the rotation Θ.

For reasons of compatibility in the assumed statical system the rotation in the span Θ_{sp} must be equal to the rotation over the support Θ_{sup}. Up to the cracking moment the stiffness along the beam length is almost constant and the moments are distributed according to the theory of elasticity. After cracking the stiffnesses in the span and over the support are approximately proportional to the corresponding area of reinforcement.

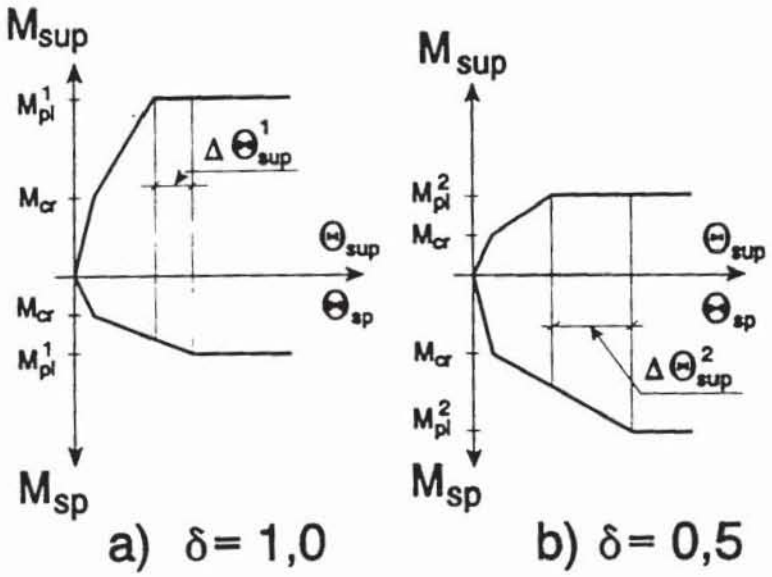

Figure 4: Development of the moment in the span and over the support as a function of the rotation depending on the moment redistribution (schematic) (after Macchi (1976))

If the beam is designed according to the theory of elasticity, the stiffness in the cracked state over the support is about twice the value of the span. Therefore the support moment increases faster than the moment in the span and reaches first the yield moment (Fig. 4a). To reach the assumed failure load, the reinforcement in the span must yield as well. Therefore a plastic rotation θ^1_{pl} ($\equiv\Delta\theta^1_{sup}$) must occur in the plastic hinge over the support (Fig. 4a), even for a beam designed according to the theory of elasticity.

If the reinforcement over the support is designed for 50 % of the elastic support moment only, after cracking the stiffness over the support is only about 50 % of the value valid for the span. However, because of the small area of reinforcement over the support, this reinforcement will yield much earlier than in the span. Therefore, to reach the yield moment in the span, a much larger plastic rotation θ^2_{pl} ($\equiv\Delta\theta^2_{sup}$) must occur than in the case of an elastic design of the beam (Fig. 4b).

The non-linear behavior of reinforced concrete structures is taken into account in MC 90 in Chapter 5 on Structural Analysis. The methods in MC 90, Chapter 5, require a certain ductility of

the plastic hinges, which is mainly governed by the ductility of the reinforcement. Therefore a certain ductility of the reinforcement is required by MC 90. In the following the methods for the structural analysis allowed by MC 90 and the ductility requirements for reinforcing steel will be discussed.

2 Structural analysis according to MC 90

2.1 General

Structural elements can be classified as

- one dimensional when one dimension is much larger than the other two (e.g. columns, beams)
- two dimensional when one dimension is relatively small compared with the others (e.g. slabs, walls, deep beams)
- three dimensional when no dimension is largely prevailing

The structural analysis of three dimensional elements is not covered in Chapter 5 of MC 90.

Any structural analysis must satisfy the equilibrium conditions. In general the compatibility conditions must be satisfied in the limit state considered. In cases where verification of compatibility is not directly required, suitable ductility conditions should be satisfied and adequate performance under service conditions should be ensured.

In general, the equilibrium conditions are formulated for the undeformed system. Only in case of slender structures the influence of deformations on action effects (second order effects) shall be considered.

The overall analysis of a structure can be performed according to the following methods:

- non-linear analysis
- linear analysis

- linear analysis with redistribution
- plastic analysis

If in the structural analysis the non-linear behavior is taken into account, it must be ensured that only a bending failure may occur and all other failure modes (e.g. shear failure, bond failure) are excluded. If the failure is not caused by bending, the available plastic rotation will be reduced significantly and brittle failure may occur before reaching the assumed bending capacity (Michalka (1986)).

2.2 Beams and frames

2.2.1 Non-linear analysis

The structural analysis is defined as non-linear, if a non-linear behavior is assumed for the materials. Second order effects may or may not be taken into account. Equilibrium and compatibility conditions can and should be satisfied in the calculation procedure.

In this approach the non-linearity arising from non-linear material properties of steel and concrete, cracking, bond slip and second order effects are taken into account in the response relationship (stiffness) of a section or an element. The method generally requires an initial definition of the geometry of the structure and of the reinforcement.

The advantage of the non-linear analysis is that it gives a realistic description of the physical behavior of the structure (distribution of deflections and internal forces) and it uses the same material laws for the static analysis and the local verification (member design). Therefore the method is considered in MC 90 as a reference for other more simplified approaches.

Disadvantageous is that superposition of different load cases is not possible. Therefore the effort for the static analysis will be larger than for methods based on the theory of elasticity.

Non-linear analysis is often done by the method of finite elements with layered elements or beam elements. The use of layered elements requires relatively much computer time. This time can be reduced considerably when employing beam elements. Their stiffness is described by a mean moment-curvature relationship. Their calculation is shown in Fig. 5.

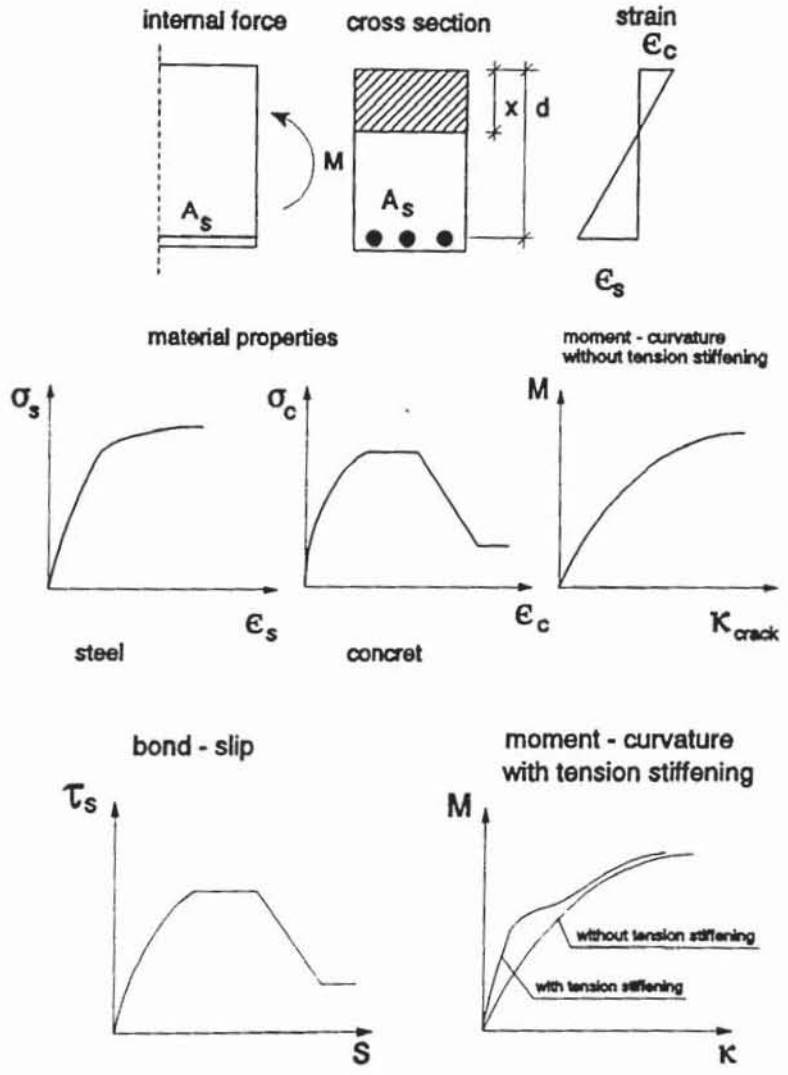

Figure 5: Calculation of the mean moment-curvature relationship (schematic) (after Kreller (1989))

Starting from the geometry of the cross section, the reinforcement layout and the material laws for concrete and steel and assuming that plane sections remain plane, the moment-curvature relationship valid for the uncracked and cracked section is obtained. By taking into account tension stiffening effects due to contribution of concrete between cracks, e.g. according to MC

90, Section 3.2, or by solving the differential equation of bond using realistic bond stress-slip laws according to MC 90, Section 3.1, one gets the mean moment-curvature relationship. With these relationships the distribution of internal forces along the structure can be calculated in an iterative way (Fig. 6). Imposed deformations can be applied at any arbitrary load step.

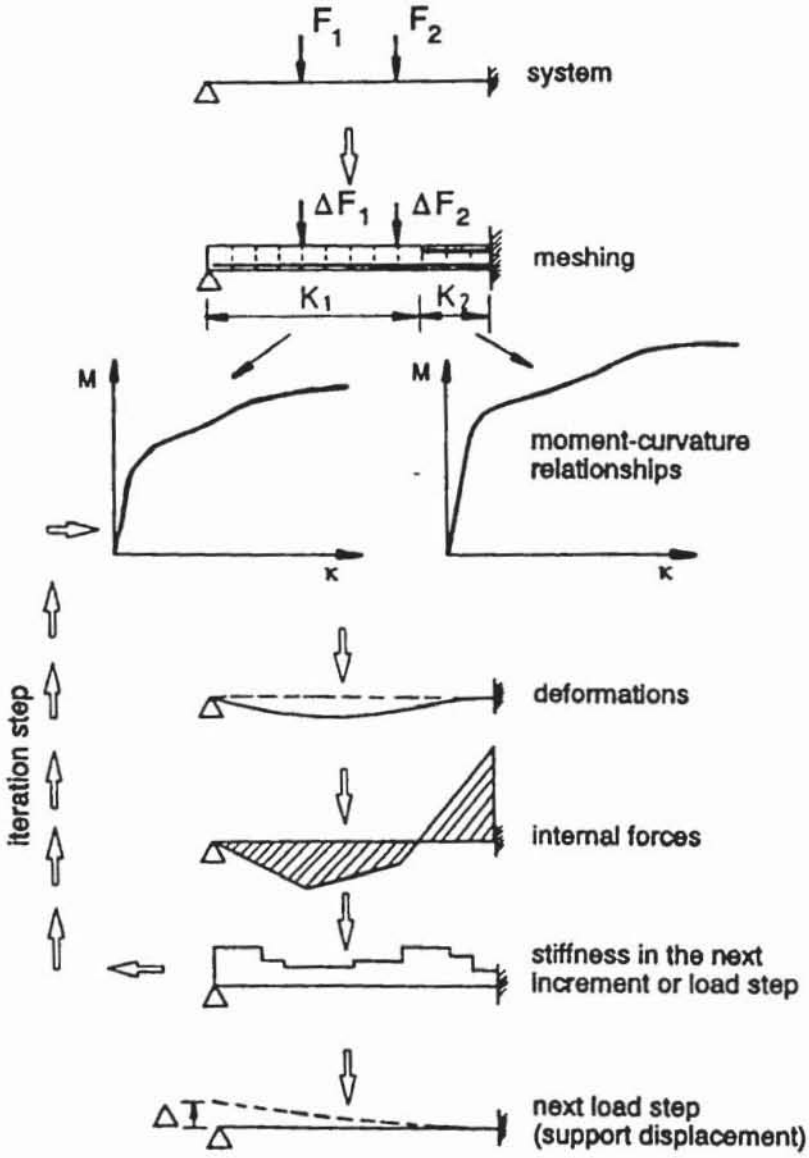

Figure 6: Iterativ procedure for the non-linear analysis of reinforced concrete structures (after Kreller (1989))

When using realistic constitutive laws for the materials (especially for the reinforcement after yielding and for the bond behavior), the behavior of reinforced concrete structures can be predicted with sufficient accuracy. This can be seen from Figs. 7 and 8.

In Fig. 7 the midspan deflections of a well confined column loaded by a normal force and a bending moment are plotted as a function of the applied load. Up to the maximum load in the ascending branch the calculated and measured deflections agree rather well.

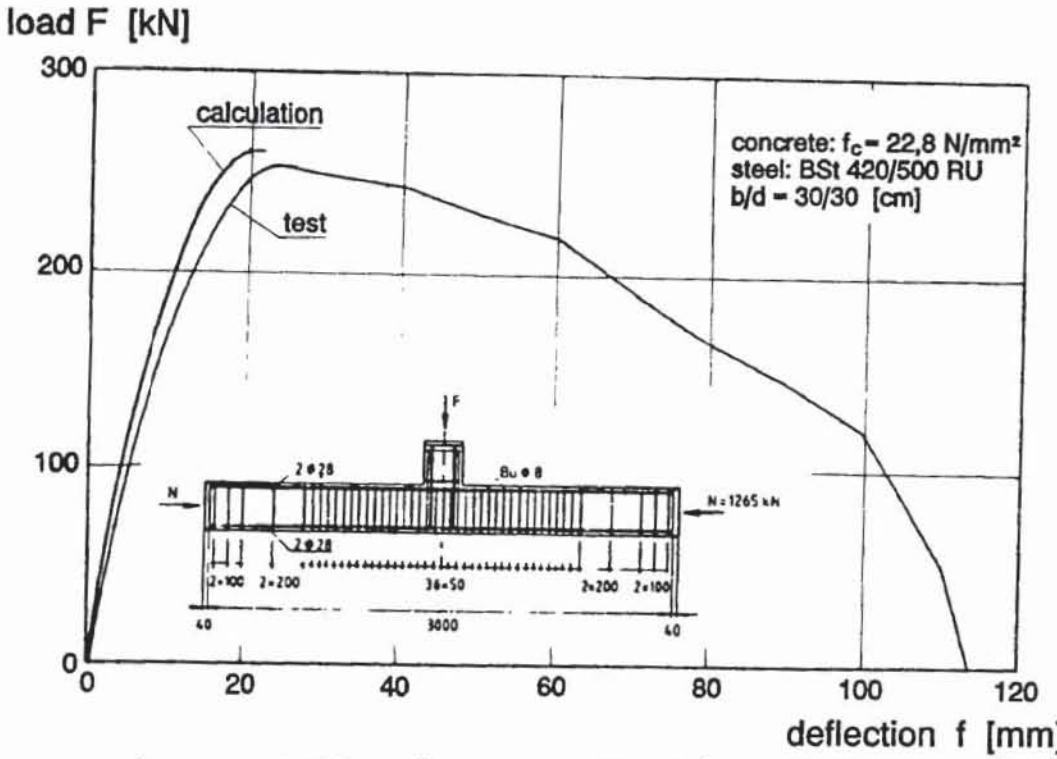

Figure 7: Midspan deflection as a function of the applied load according to tests by Steidle, Schäfer (1986) and calculations by Kreller (1989)

In Fig. 8 the test result of a continuous three span girder are compared with calculations using the discribed non-linear programm with finite beam elements.

In the first test the girder was subjected to two concentrated loads in the midspan. In the second test an imposed displacement of 3 mm of the outer supports was applied before loading the beam. Both beams were designed according to the theory of elasticity with a moment redistribution of 50 % from the supports into the field. The employed reinforcement was rather ductile.

As one can see, the calculated development of the support and midspan moment agrees very well with the measured results. Due to the ductility of the support section, at failure the moment

caused by the imposed deformation is reduced to almost zero. Therefore the bearing capacity of the girder with an imposed deformation is nearly the same as for the girder subjected to point loads only.

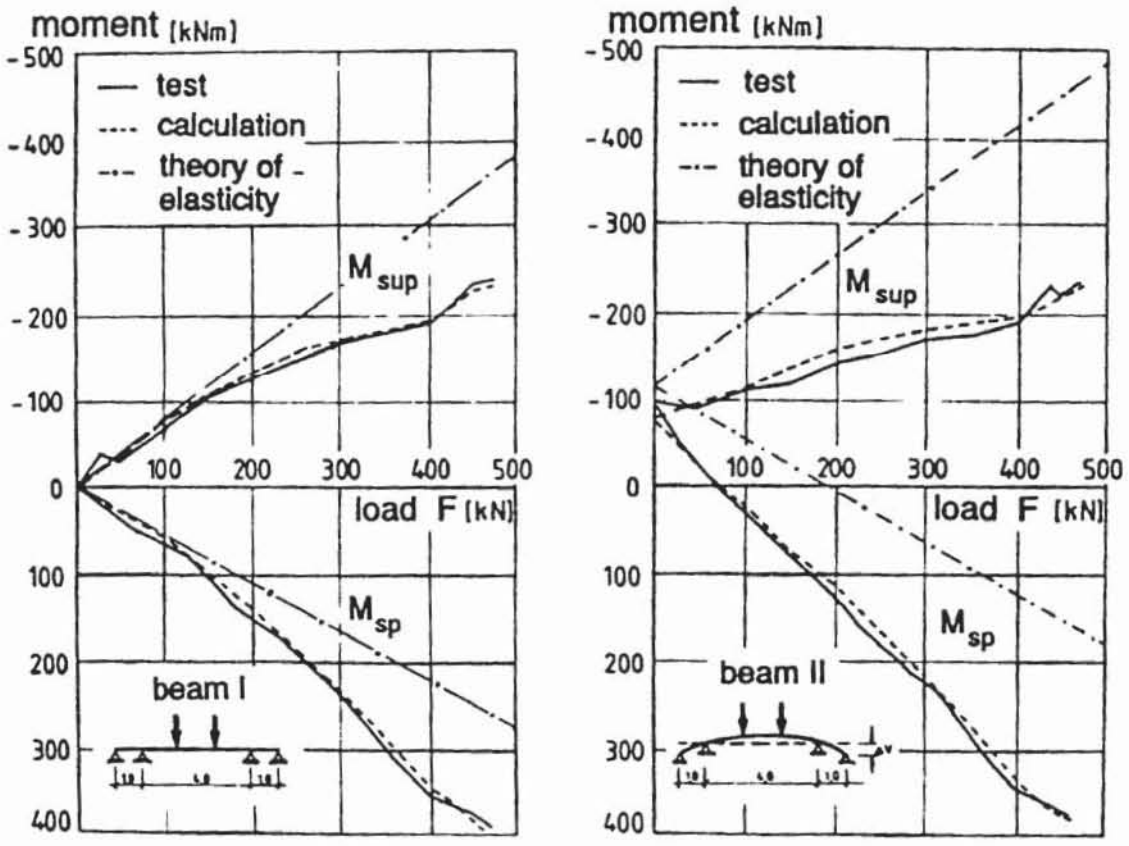

Figure 8: Support and span moments as a function of the applied load according to tests by Schlaich, Schäfer, Woidelko (1982) and calculations by Kreller (1989)

In a simplified approach, the mean moment-curvature relationship (see Fig. 5) can also be obtained from MC 90, Section 3.6. However, the relationship according to Section 3.6 seems to be less accurate than the procedure proposed above, because Section 3.6 does not agree well with Section 3.2, which is based on the local bond stress-slip relationship given in Section 3.1.

In the examples shown in Figs. 7 and 8 average material properties were taken to calculate the average failure load. According to MC 90 for design purposes, after design yield is attained in critical regions, design values of the material properties should be used both for the analysis and for the resistance

determination. The moment-curvature relationship after yielding can be obtained assuming an affinity between the characteristic values. However, according to Eibl (1991) this approach may not yield realistic results in several cases.

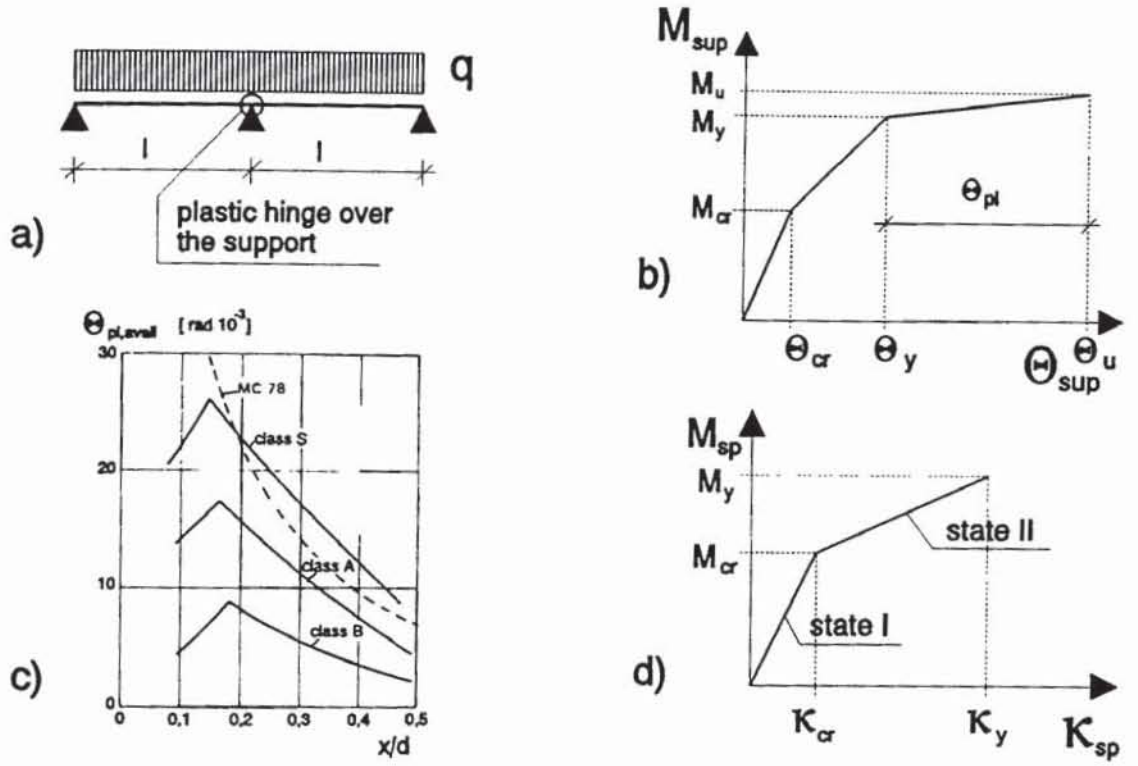

Figure 9: Assumptions for the simplified non-linear analysis according MC 90, Section 5.4.1.2

A further simplification is to assume that the total plastic rotation is concentrated in plastic hinges (Fig. 9a,b) (Macchi (1979)). The possible plastic rotation is taken from Fig. 5.4.2 of MC 90 (see Fig. 9c) as a function of the relative depth of the neutral axis in the critical section. Parameter is the steel class in respect to its ductility. Three ductility classes are distinguished: class S, class A and class B. The rationale for this distinction and for Fig. 9c will be given in chapter 3. The rotation in the span is calculated by integrating simplified bi-linear moment-curvature relationships (Fig. 9d). Equilibrium and compatibility are obtained, if the rotation in the field corresponds to the rotation over the support which must be smaller than the value according to Fig. 9c. When using Fig. 9c, the value x/d must be calculated as described in section 3.4 in the explanation of Fig. 24.

2.2.2 Linear analysis

The structural analysis is defined as linear if a linear elastic behavior is assumed for the materials. The results are realistic only if the members are uncracked, because cracking may cause a moment redistribution of up to about 20 %. Linear analysis is to be applied mainly for serviceability limit states and may also be used for verifying the ultimate limit state for continuous beams and non-sway frames.

It can also be used for determining the first order loading effects for sway frames, provided that the reduction in bearing capacity due to second order effects does not exceed the limit defined in MC 90, Section 6.6.13.

At the ultimate limit state a linear analysis cannot always satisfy the conditions of compatibility in view of the invalidity of the assumptions relating to the material behavior. Therefore the beam shall be capable of sufficient plastic rotation to prevent local rupture before the calculated moment distribution has been attained.

Because the available plastic ductility decreases with increasing ratio x/d (see Fig. 9c), the maximum value of x/d is limited for continous beams and non-sway frames:

For type S and type A steel:

- for concrete grades C 12 to C 35: $x/d \leq 0{,}45$
- for concrete grades C 40 to C 80: $x/d \leq 0{,}35$

For type B steel:

- for concrete grades C 12 to C 80: $x/d \leq 0{,}25$

According to Fig. 9c, the plastic ductility is lower for type A steel than for type S steel. Therefore different limiting values for the ratio x/d should be given for the two steel types. However, this was neglected for reasons of simplicity. The limiting values given for type A and S steel correspond to the values given in MC 78. The influence of the concrete strength seems to

be overestimated, because neither the available plastic rotation (see Fig. 9c) nor the required plastic rotation (see Fig. 26) are much influenced by the concrete strength.

The ductility is increased by transverse reinforcement. The ratio x/d can be reduced by means of suitable compression reinforcement.

According to the opinion of the authors the requirements are valid for beams without significant normal forces. They should not be applied to columns with high normal forces.

2.2.3 Linear analysis followed by limited redistribution

The structural analysis is defined as linear with redistribution, if the action effects derived from a linear analysis are redistributed in the structure.

For the verification in the ultimate limit state, it is allowed to reduce the moments in the sections subjected to the highest action effects resulting from a linear analysis using the stiffness of the uncracked section, provided that in the other sections the moments are increased to maintain equilibrium. All the consequences of the assumed redistribution and of the possible scattering of its value should be taken into account in the verification procedure concerning shear, anchorage of the bars and cracking. In particular, the length of the reinforcing bars shall be sufficient to prevent any other section becoming critical.

The required plastic rotation increases with increasing degree of moment redistribution (see chapter 3). The available plastic rotation decreases with increasing ratio x/d (see Fig. 9c). Therefore, to maintain compatibility, the reduction coefficient δ to be used for multiplying the moments in the sections subjected to the highest moments should satisfy the following conditions (see Fig. 10):

For type S and type A steel:

- for concrete grades C 12 to C 35: $\delta \geq 0{,}44 + 1{,}25 \cdot x/d$ (1a)
- for concrete grades C 40 to C 60: $\delta \geq 0{,}56 + 1{,}25 \cdot x/d$ (1b)
- for continuous beams and non-sway frames: $0{,}75 \leq \delta \leq 1{,}0$
- for sway frames: $0{,}90 \leq \delta \leq 1{,}0$

For type B steel:

- for concrete grades C 12 to C 60: $\delta \geq 0{,}75 + 1{,}25 \cdot x/d$ (1c)
  $0{,}90 \leq \delta \leq 1{,}0$

The above equations are valid for beams with straight axes in the horizontal plane only, because in curved beams flexural yielding may produce a sudden increase of torsion, which can lead to a brittle failure before the redistribution of flexural moments is fully exploited.

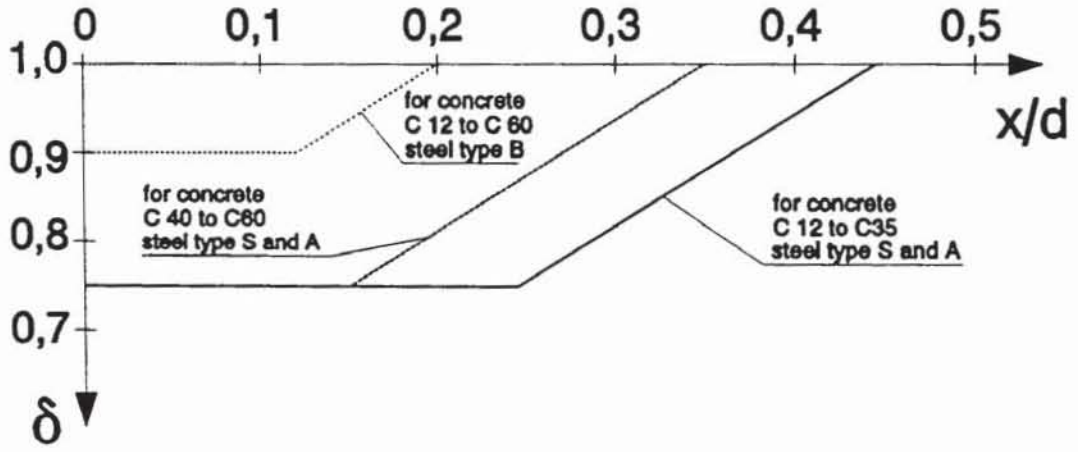

Figure 10: Allowable degree of moment redistribution according to MC 90

Post-tensioned steel may be assimilated to type A steel and pre-tensioned steel to type B steel. The reason for this is, that prestressing steel is generally not very ductile. However, post-tensioned steel generally has a relatively poor bond behavior and the available plastic rotation increases with decreasing bond properties (see chapter 3). The above assumption is a rough estimate only and currently research is going on at the University of Stuttgart to give more precise definitions of the required ductility of prestressing steel.

According to Fig. 9c, the available plastic rotation depends on the type of steel and is independent of the concrete quality. This is not well reflected by the actual equations for the allowable degree of moment redistribution, which for type S and A steel were taken from MC 78.

2.2.4 Plastic analysis

The structural analysis is defined as plastic if one of the three basic theorems of plasticity: Upper bound, Lower bound and Uniqueness is met, assuming a rigid-plastic or elastic-plastic behavior for the materials.

Plastic analysis is allowed only if sufficient ductility for the attainment of the assumed mechanism is ensured. Therefore it should be verified that the required plastic rotations in the plastic hinges, for the assumed mechanism, are less than the limiting plastic rotation θ_{pl} given in MC 90, Fig. 5.4.2 (see Fig. 9c). The method is not allowed when consideration of second order effects is required, for sway frames or if type B steel is used. Type B steel is excluded, because it has a rather limited ductility and there exist no experimental investigations for structures designed according to the theory of plasticity and reinforced with type B steel.

2.3 Slabs

In principle, the same methods of analysis are allowed for slabs as for beams. When performing a plastic analysis, the following conditions must be met to ensure sufficient rotation capacity:

a) Type A or S steel must be used, because no experimental or theoretical investigations have been performed with type B steel as reinforcement.

b) The tensile reinforcement at any point and in any direction should not exceed one half of that which corresponds to a

section for which the ULS in bending is characterised by the following strains: $\epsilon_y=f_y/E_s$ and $\epsilon_c=-0,0035$

c) For slabs with fixed supports or continuous slabs the ratio of the support moments to the midspan moments should normally not be less than 0,5 or more than 2.

d) The minimum reinforcement must be the same as for beams to prevent a brittle failure after crack formation.

e) For ribbed slabs it may be necessary also to verify the shear capacity of the shear reinforcement and of the compression zone considering the crack depth to prevent a shear failure before reaching the ultimate bending strength. However, this condition must be met for any non-linear analysis (see chapter 2.1).

2.4 Deep beams and walls

The forces acting in the middle plane of a deep beam may be determinate by applying either:

a) linear analysis based on the theory of elasticity,
b) statically admissible stress fields in accordance with the Lower bound theorem of limit analysis or
c) non-linear analysis.

Often the analysis is done by strut and tie models. An example is given in Fig. 11.

In this case a lower bound solution of limit analysis is considered. For the structure and its loads an equivalent truss may be investigated, consisting of concrete struts and arches as compression members and of steel ties formed by the reinforcement as tensile elements and their connections (nodes). The model should follow the elastic stress field as closely as possible. The equilibrium model may be applied for verifying the ULS and also for the SLS, provided that the truss model is close

to the results of the linear analysis. According to MC 90, Section 5.6.3, this method is not allowed if type B steel ist used, because a certain ductility is required, which may not be ensured by this steel.

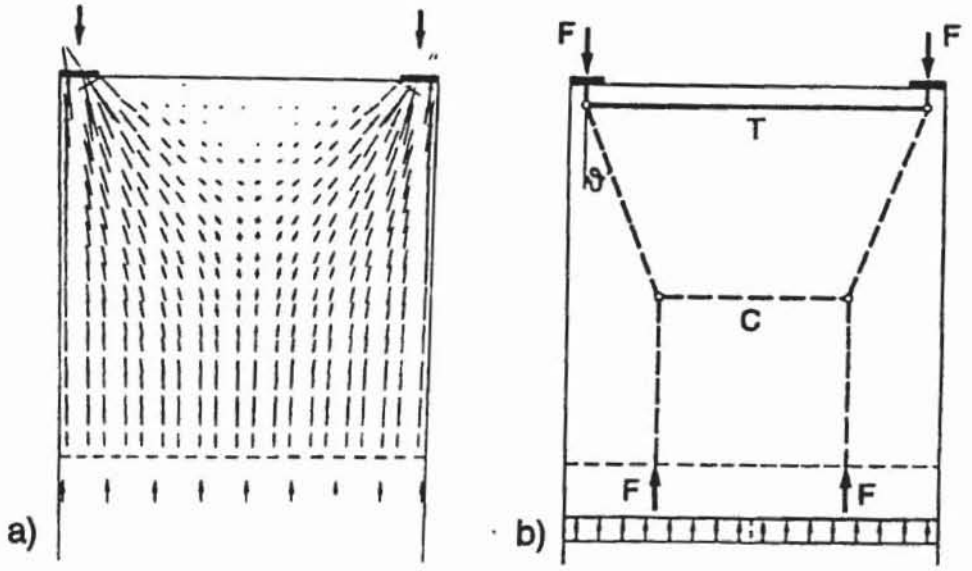

Figure 11: Deap beam: principal stresses (Fig. 11a) and corresponding strut and tie model (Fig. 11b) (after Schlaich, Schäfer (1989))

For a more refined analysis non-linear stress-strain relations may be taken into account by applying numerical methods, e.g. finite elements, for two-dimensional plane structures. The analysis then gives results for the serviceability as well as for the ultimate limit states.

3 Ductility requirements of reinforcing steel

3.1 General

According to chapter 2, sufficient ductility is needed whether the structural analysis is performed according to a linear, non-linear or plastic analysis. This ductility is mainly ensured by the ductility of the reinforcement.

It should be noted that ductility of the reinforcement is needed also for other reasons:

- In the section verification for bending moments a bi-linear stress-strain diagramme with in principle unlimited steel strains is assumed.

- Often the effects of imposed deformations are not taken into account in the structural analysis. Therefore ductility is needed to decrease the internal forces due to imposed deformations to a neglectable degree.

- In the shear design or in the design of so-called D-regions strut and tie models are employed. The tension stresses are concentrated in the assumed tension ties and taken up by the reinforcement. Because the direction of the ties might deviate from the direction of the tensile stress field, plastic behavior of the reinforcement is needed to ensure the assumed bearing behavior of the truss.

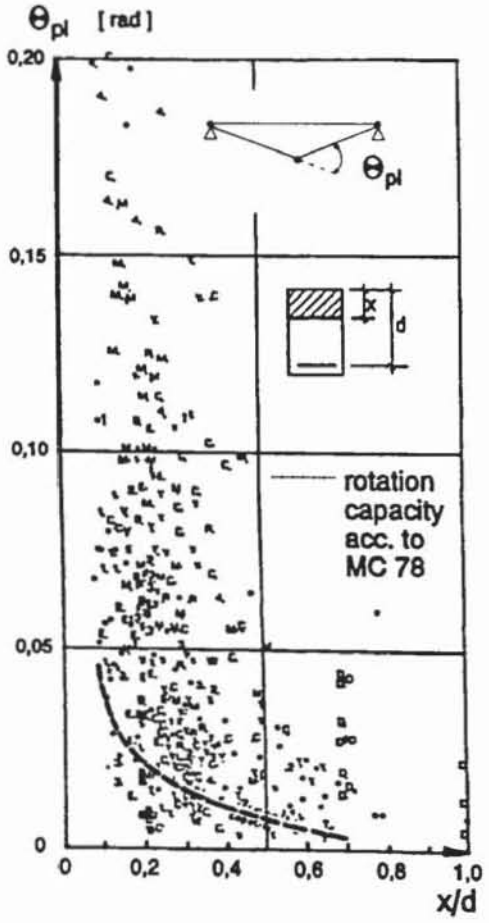

Figure 12:
Plastic rotation capacity of reinforced concrete hinges (after Siviero (1976))

In MC 78 the available plastic rotation was given in a figure as a function of the relative depth of the neutral axis x/d (Fig. 12). This figure was proposed by Siviero (1976).

He plotted the rotation capacity measured in about 350 tests on beams performed approximately between 1960 and 1970 as a function of the ratio x/d. The allowable plastic rotation - shown in Fig. 12 as dotted line - was evaluated by a statistical analysis of the data and shall represent the 5%-fractile of the test results. The scatter of the test results is very large, indicating that the plastic rota

tion capacity is influenced also by other parameters than x/d. Therefore a statistical analysis of the data may be questionable. Furthermore the employed steel was rather ductile with a ratio $f_t/f_y \approx 1,4-1,8$ and a strain at maximum load $\epsilon_u > 10$ %. In addition the bond behavior of the bars used in some tests was rather poor (smooth bars or deformed bars with a small value for the related rib area). All these factors will contribute to a rather large plastic rotation capacity.

In Fig. 13 the stress-strain relationships of reinforcing bars used today in Germany are shown. Similar steels are also used in other European countries. These curves were found by evaluating a large number of quality control tests from several steel mills (Eligehausen, Langer, Kreller (1984)).

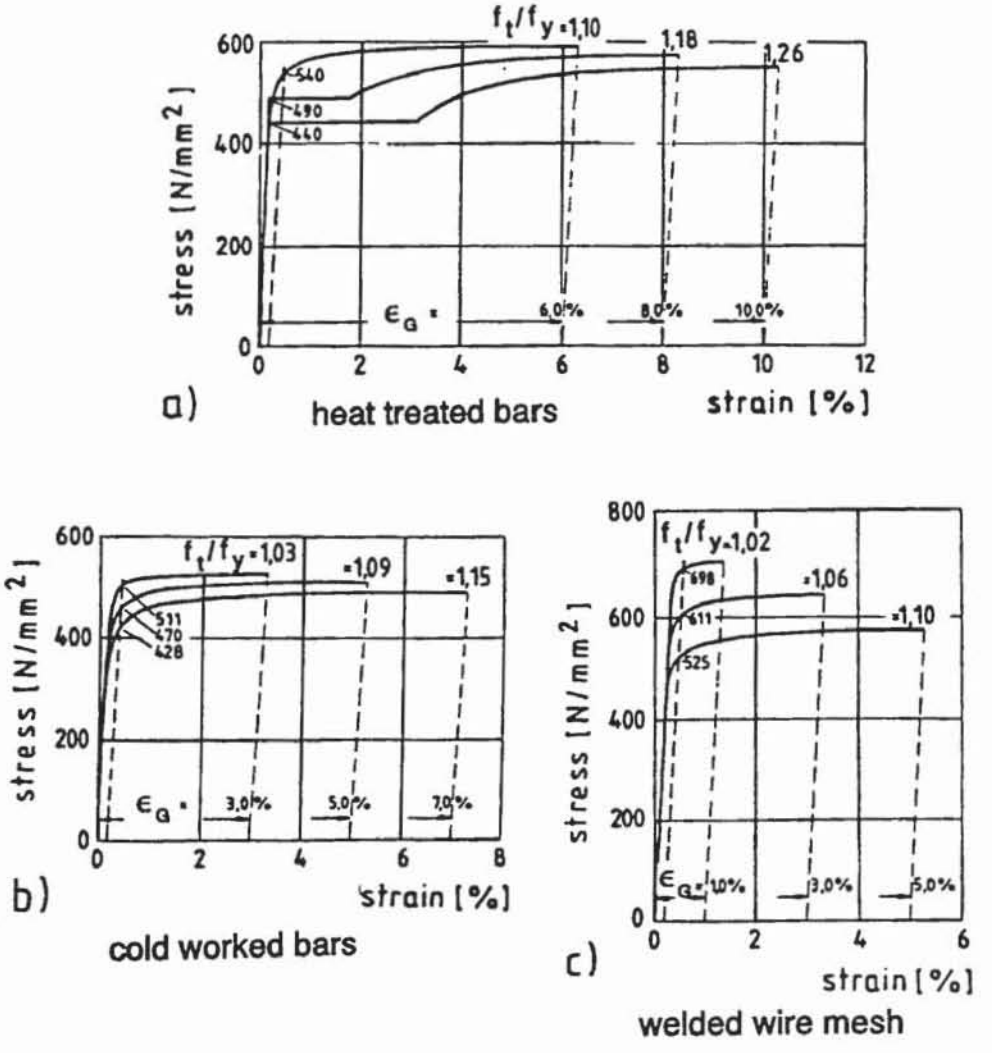

Figure 13: Stress-strain relationship of reinforcing steel produced in Germany (after Eligehausen, Langer, Kreller (1984))

The upper and lower lines are approximate limits of the scatter expected in practice. It can be seen that modern reinforcing steel is less ductile than the steel employed in the above described tests. This is especially true for cold worked bars and for welded wire mesh produced from cold worked wires. Furthermore modern deformed bars have a very good bond behavior.

For these reasons the plastic rotation capacity given in MC 78 may not always be reached when using modern - especially cold worked - reinforcement. To predict the available plastic rotation, a numerical model was developed (Langer (1987)), based on the work by Dilger (1966) and Bachmann (1967). This model is briefly described in the following. For details see Langer (1987).

3.2 Numerical model

The numerical model is summarized in Fig. 14.

First the moment-curvature or tensile force-curvature relationship is calculated as explained before (Fig. 14f). The distribution of moments or tensile forces, respectively, along the beam is calculated taking into account the width of the loading plate (Fig. 14h). The load is increased until the ultimate moment previously calculated is reached. That means, that the increase of the plastic rotation in the descending branch of the load-deflection curve (compare Fig. 1) is neglected. If shear cracks must be expected, the shifting of the tensile force compared to the M/z-line (M = Moment, z = lever arm) (truss analogy) is taken into account assuming an angle of the inclined compression struts according to Dilger (1966) (Fig. 14h, right side of the diagramm). From the tensile force distribution and the tensile force-curvature relationship the curvature in the cracks is reached (Fig. 14m). The crack distance is calculated according to Martin, Schießl, Schwarzkopf (1980). In the left side of Fig. 14h and 14m it is assumed, that no shear cracks will occur, while the right side of these digramms are valid for a beam with inclined shear cracks.

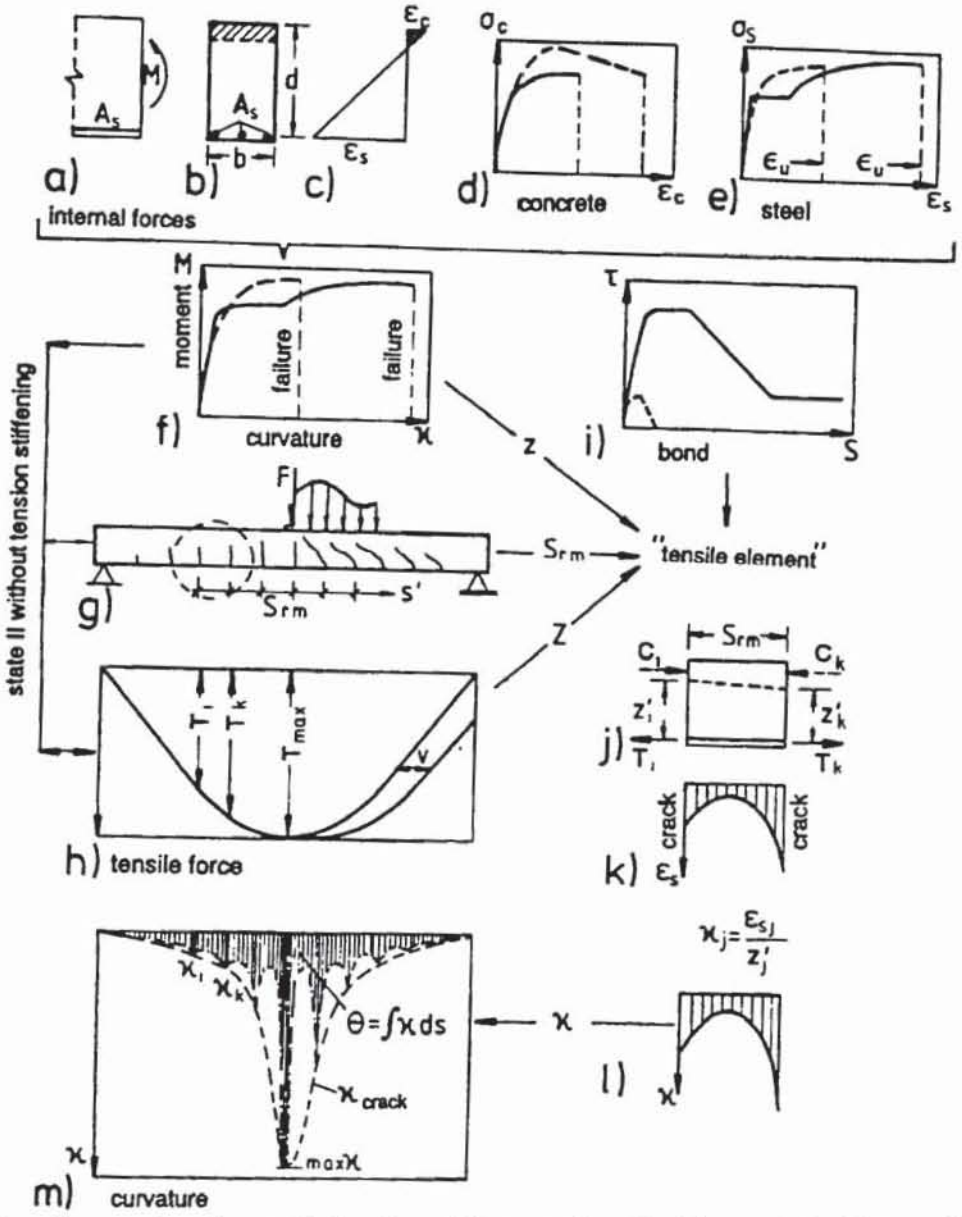

Figure 14: Numerical model for the calculation of the plastic rotation capacity (after Langer (1987))

The contribution of concrete between cracks is calculated for every section between two cracks by means of an iterative solution of the differential equation of bond, using a modified version of the program described in Ciampi et al. (1982). On the basis of the calculated steel strain distribution (Fig. 14k), the distribution of curvature between the cracks (Fig. 14l) is derived by using the distance of the tensile reinforcement to the neutral axis (Fig. 14j). Integration of these curvatures over the beam length yields the rotation capacity θ of the beam (Fig. 14m).

The plastic rotation is defined as the difference between the rotation at ultimate load and at a load causing yielding of the reinforcement at the point of maximum moment.

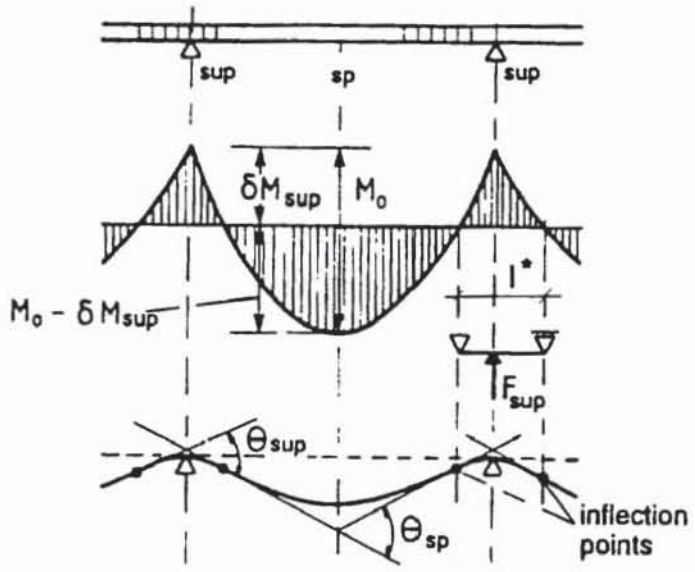

Figure 15:
Evaluation of a statically determinate beam from a statically indeterminate structure for calculating the rotation capacity over the support (after Langer (1987))

In statically indeterminate structures an statically determinate beam with a length equal to the distance between two adjacent points of zero moment is cut out of the real system (Fig. 15).

The mathematical model can yield reliable results only, if the behavior of the material is described very accurately. Therefore the stress-strain relationship of the reinforcing steel is described by a polygon with up to 30 points, which allows a very close representation of the real behavior. The assumed stress-strain relationship of the concrete agrees rather well with the proposal in MC 90, Section 2.1. The assumed bond behavior agress with MC 90, Section 3.1.1, which is based on the work described in Eligehausen et al. (1983).

To check the validity of the assumptions, the predicted response of beams was compared with available test results. In Fig. 16 the calculated and measured distribution of the residual steel elongations after unloading from maximum load are plotted. Note that in the experiment (Eifler, Plauk (1974)) the crack spacing varies, while in the calculation a constant value was assumed.

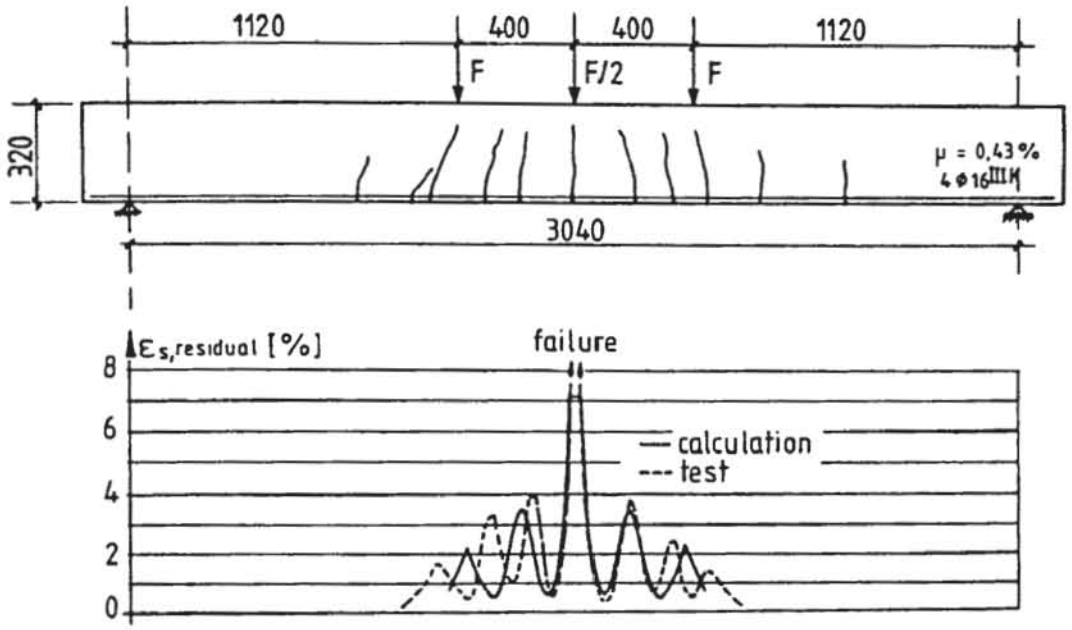

Figure 16: Residual steel strains in the area of a plastic hinge according to test (Eifler, Plauk (1974)) and calculation (Langer (1987))

Fig. 17 shows the predicted total rotation capacity of 70 beams as a function of the measured value. The data points scatter around the 45-degree line for perfect agreement. The coefficient of variation is only 17 %.

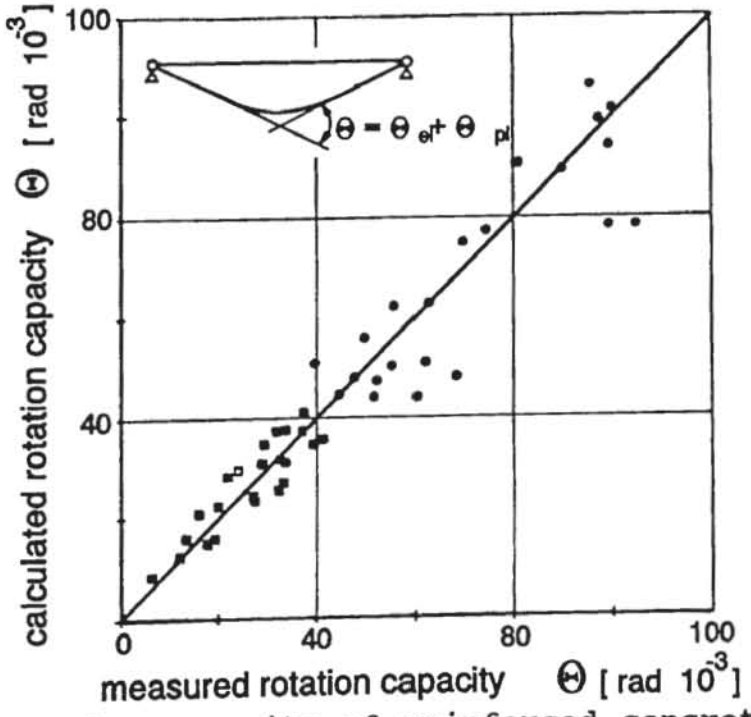

Figure 17: Rotation capacity of reinforced concrete hinges according to calculation and experiment (after Langer (1987))

In Fig. 18 the predicted and measured rotation capacities of otherwise identical beams are plotted as a function of the percentage of reinforcement. The typical roof shaped behavior found in the tests is captured quite well by the calculation.

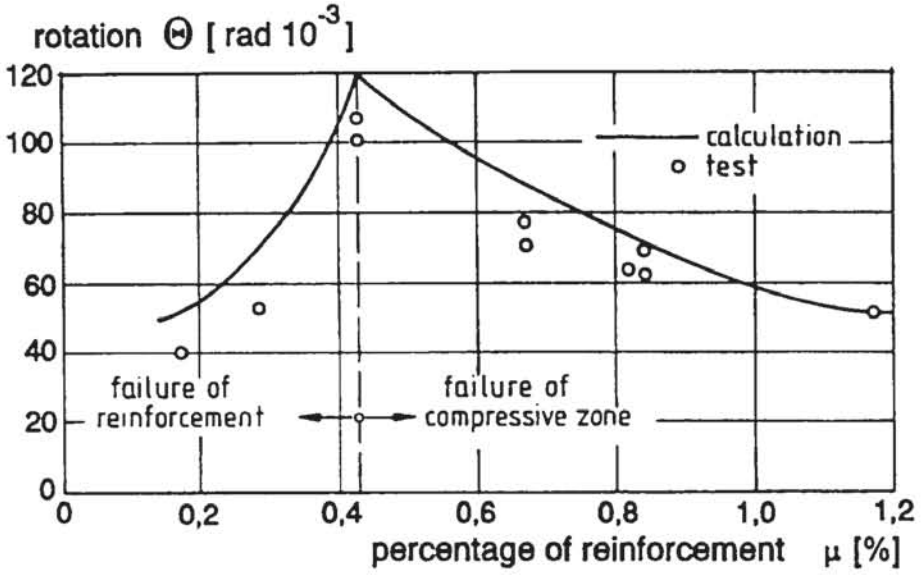

Figure 18: Influence of the percentage of reinforcement on the rotation capacity of reinforced concrete beams after tests (Eifler, Plauk (1974)) and calculation (Langer (1987))

For reinforcement percentages smaller than a critical value (which depends on the strength of steel and concrete and the shape of the cross section) the beam fails due to rupture of the reinforcement, i.e. the ductility of the reinforcement is fully utilized. For this failure mode the rotation capacity decreases with decreasing reinforcement percentage, because only fewer cracks are formed and the contribution of concrete between cracks is significant. For reinforcement percentages larger than a critical value, the beam fails due to crushing of the concrete. The steel strains are smaller than the value ϵ_{su} (ϵ_{su} = steel strain at peak load). In case of concrete failure, the rotation capacity can be significantly increased by confining the compression zone. Note, that confinement has no influence on the rotation capacity in case of steel failure.

From these figures it can be concluded that the proposed analytical model is sufficiently accurate for practical purposes.

3.3 Parameter studies

Fig. 19 shows schematically the influence of the stress-strain curve on the rotation capacity of a single span reinforced concrete beam loaded in midspan (Fig. 19a).

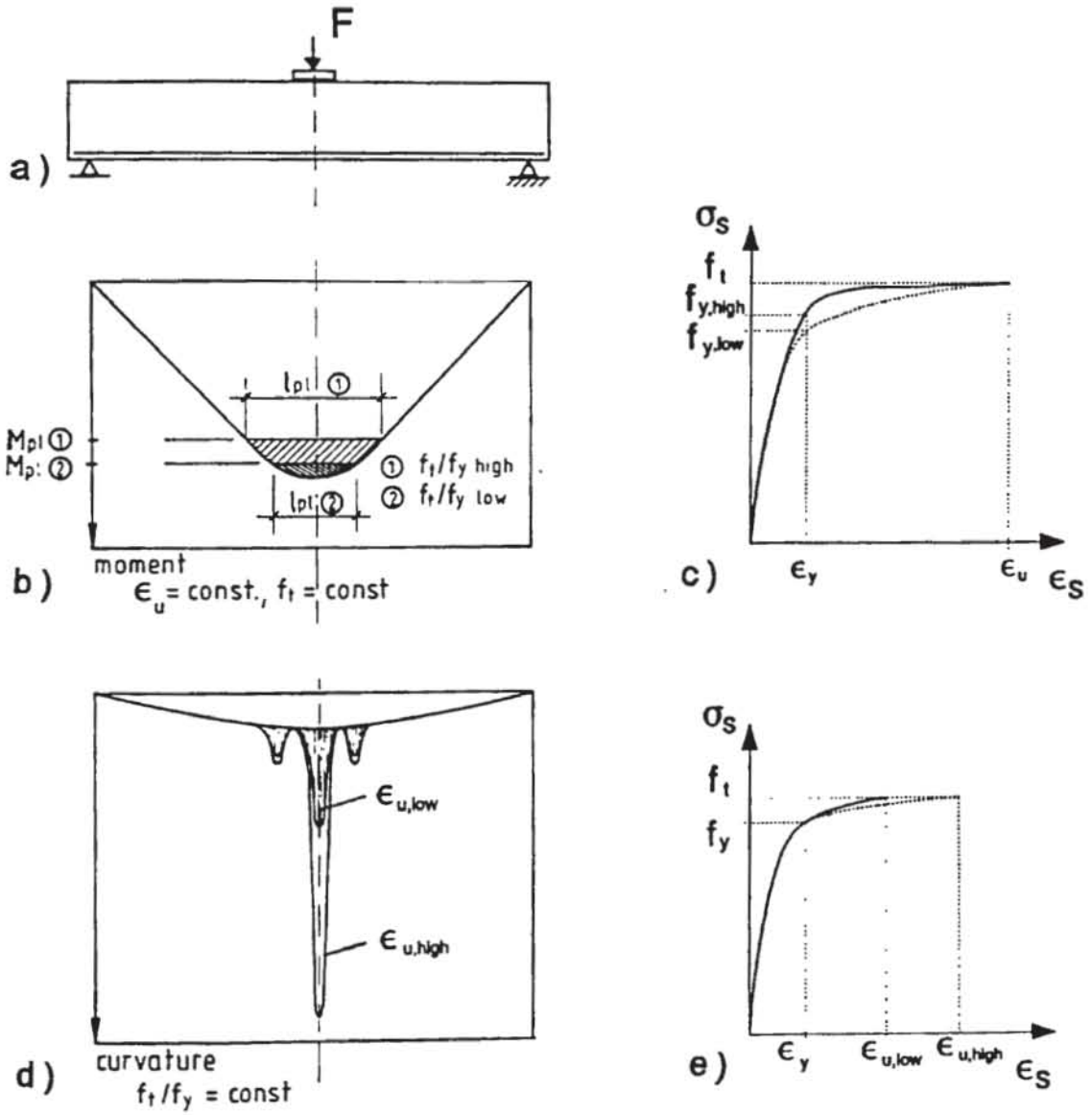

Figure 19: Influence of the stress-strain relationship of reinforcing steel on the rotation capacity of plastic hinges (after Langer (1987))

In Fig. 19b, which shows the moment distribution along the beam, the influence of the ratio f_t/f_y on the rotation capacity is investigated. It is assumed that the tensile strength of the steel and the elongation at maximum load ϵ_{su} are constant (Fig. 19c). Under these conditions the maximum section curvature and

the ultimate moment are almost constant. The plastic rotation capacity is approximately proportional to the length of the plastic zone. Because this length increases with increasing ratio f_t/f_y, the rotation capacity increases considerably with increasing ratio f_t/f_y.

In Fig. 19d, which shows the distribution of section curvature along the beam length, a constant ratio f_t/f_y, but different values for the elongation at maximum load ϵ_{su} are assumed (Fig. 19e). In this case the length of the plastic zone is almost constant. However, with increasing elongation ϵ_{su} the maximum section curvature increases, resulting in an increasing rotation capacity.

The reinforcement percentage of the beam investigated in Fig. 19 is relatively small ($\mu=A_s/b\cdot d=0,003$) and therefore the beam will fail by rupture of the steel. For higher reinforcement ratios leading to a concrete failure the rotation capacity will also increase with increasing ratio f_t/f_y, but will be less influenced by the elongation ϵ_{su}.

In practice for a certain type of reinforcement (e.g. cold worked bars) the elongation ϵ_{su} increases with increasing ratio f_t/f_y (compare Fig. 13). The combined effect is investigated in Fig. 20 using the same beam as in Fig. 19.

Plotted is the plastic rotation capacity as a function of the shape of the stress-strain diagram. The assumed stress-strain relationships (Fig. 20a) cover approximately the range valid for welded wire fabric produced in Germany (compare Fig. 13c). The plastic rotation capacity of the beam reinforced with the more ductile steel 1 is about 3 times larger than for steel 3 (Fig. 20b).

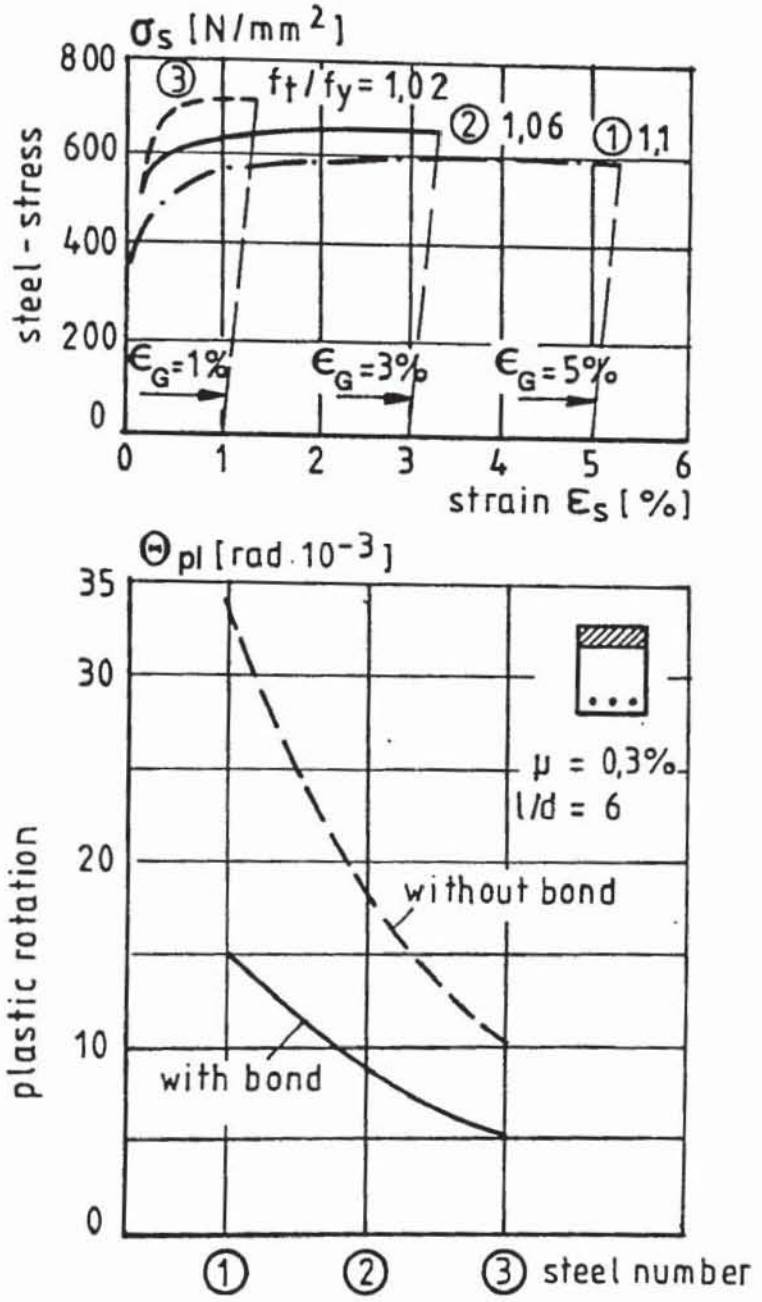

Figure 20: Influence of the stress-strain relationship of reinforcement on the plastic rotation capacity (after Langer (1987))

From Fig. 20 the significant influence of bond between bars and concrete on the plastic rotation can also be seen. While the dotted line is valid for the so-called naked state (no contribution of concrete between cracks), the full line takes the influence of bond (tension stiffening) into account. Under otherwise constant conditions the plastic rotation capacity is reduced by about 60 % due to bond compared to the "naked state". This can be explained by the fact that for steel strains $\epsilon_s > \epsilon_y$

small differences in forces caused by the bond action result in large changes of the steel strains.

The influence of bond is especially pronounced for steel with a low ratio f_t/f_y.

It is smaller for higher percentages of reinforcement but still significant (see Fig. 21).

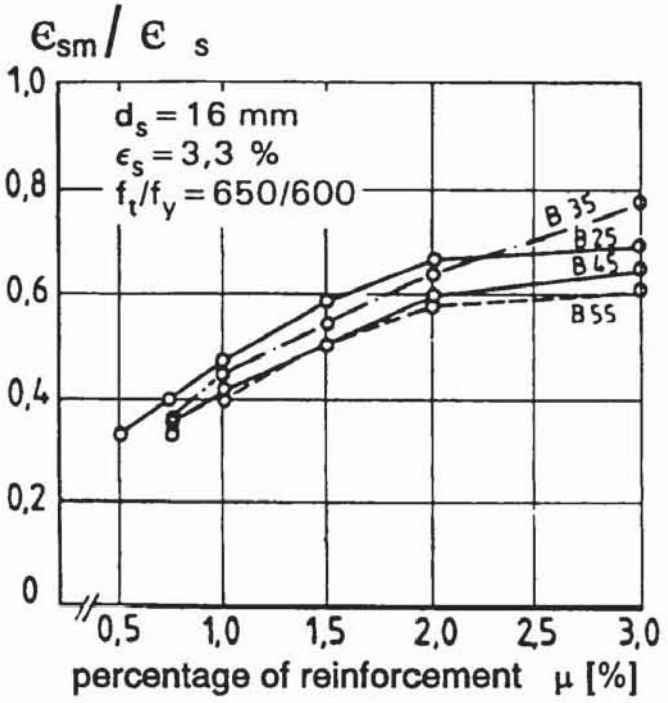

Figure 21: Ratio mean steel strain to steel strain in the crack ϵ_{sm}/ϵ_s as a function of the reinforcement percentage (after Kreller (1989))

The importance of the steel behavior on the rotation capacity has also been pointed out by Dilger (1966) and Bachmann (1967).

The rotation capacity is further influenced by confinement of the concrete compression zone (in case of a concrete failure), the width of the loading plate and the slenderness of the beam (Fig. 22).

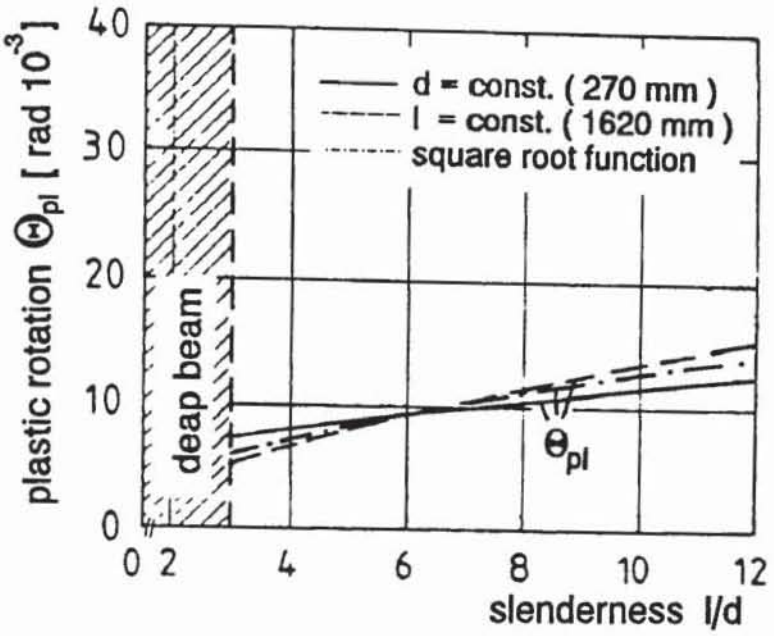

Figure 22: Influence of the slendernes on the rotation capacity (after Langer (1987))

Another important influencing factor is how the load is applied either through a column or a steel plate. In the first case the rotation capacity is only about 45 % of the value valid for a beam with loads applied through a steel plate. This can be seen in Fig. 23 which summarizes the results of tests performed by Rao et al. (1971).

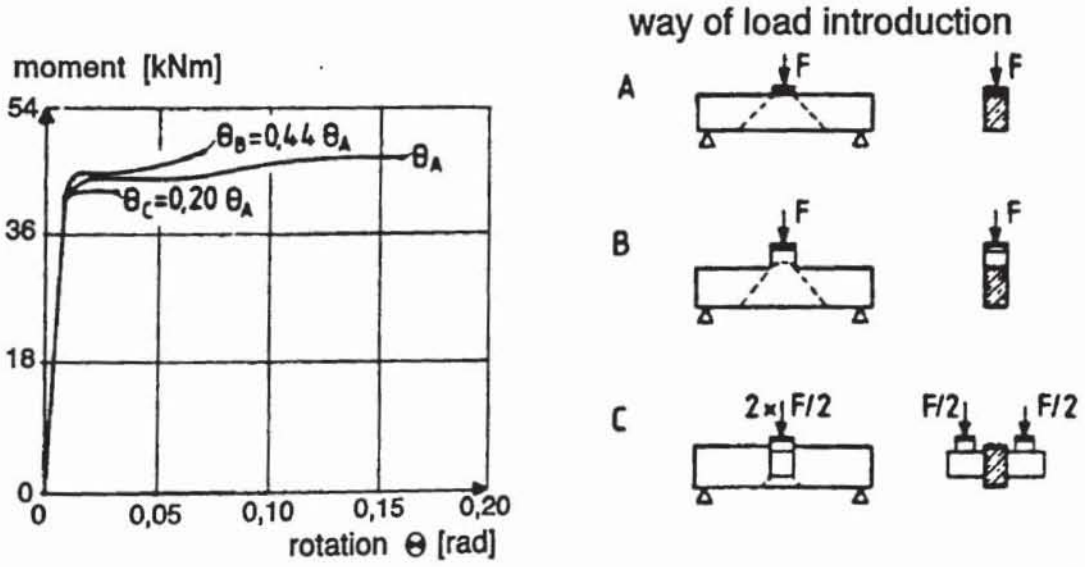

Figure 23: Influence of load introduction on rotation capacity of reinforced beams tested by Rao et al. (1971)

3.4 Available plastic rotation and allowable degree of moment redistribution

Because the plastic rotation capacity is significantly influenced by the stress-strain relationship of steel, three ductility classes have been introduced in MC 90. The following values must refer to the 5%-fractile:

class S: $(f_t/f_k)_k \geq 1{,}15$ and $\epsilon_{uk} \geq 6$ %

class A: $(f_t/f_k)_k \geq 1{,}08$ and $\epsilon_{uk} \geq 5$ %

class B: $(f_t/f_k)_k \geq 1{,}05$ and $\epsilon_{uk} \geq 2{,}5$ %

These steel classes were defined after an intensive discussion in the responsible Commission VII "Reinforcing Steel". They take into account the current production methods for hot rolled and heat treated steel (class S), cold worked bars and bars of heat treated steel made from coils (class A), welded wire mesh produced from cold worked wires without additional heat treatment after welding and bars of cold worked steel made from coils (class B).

This distinction of the different types of steel in respect to ductility is necessary, if the non-linear behavior of structures shall be exploited in the structural analysis. However, it may cause serious problems on site, because the marking of the reinforcement to destinguish different ductility classes may be difficult and hence another type of steel may be placed in the formwork than assumed in the design. Therefore it is desirable to improve the ductility of Type B steel to a generally acceptable degree so that for all non seismic applications only one type of steel can be employed.

In Fig. 24 the available plastic rotation is plotted as a function of the ratio x/d. For comparison the rotation capacity according to MC 78 is shown as well.

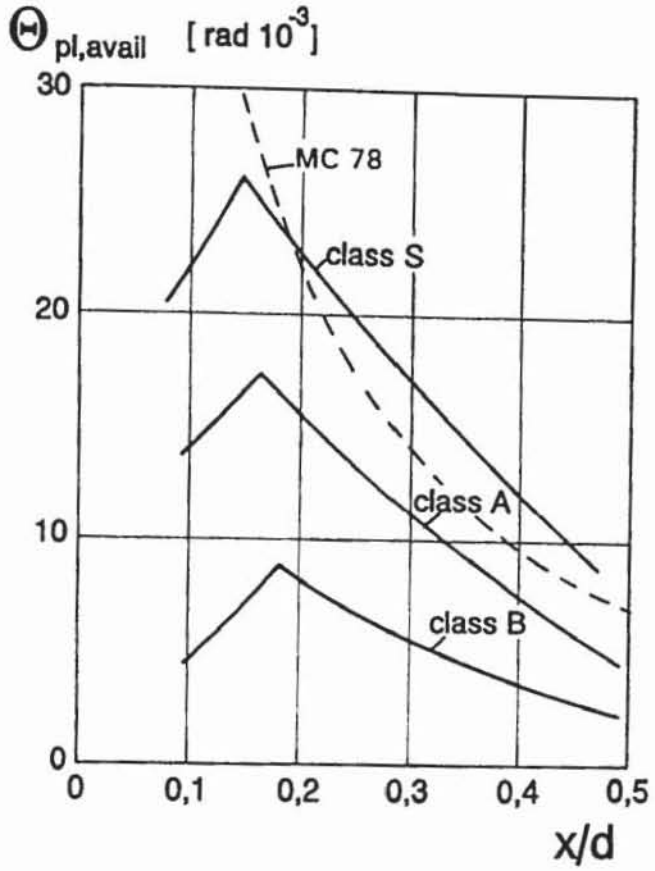

Figure 24: Available plastic rotation as a function of the ratio x/d for the three different steel classes defined in MC 90 (see Figure 5.4.2 in MC 90 and Fig. 9c)

The calculated values are valid for the following parameters:

- Reinforced concrete beam or slab with tension and shear reinforcement, but without compression reinforcement. It was assumed that sufficient shear reinforcement was provided to prevent a shear failure. The statically determinate beam or slab was cut out of a continuous beam or slab and should represent the region over the support (compare Fig. 15). The slenderness of the statically determinate beam was assumed as $l^*/d=6$. Depending on the degree of moment redistribution the slenderness of the continuous beam is $l/d \approx 14$ ($\delta=1,0$) to $l/d \approx 27$ ($\delta=0,6$).

- Reinforcement with f_y=500 N/mm². The tensile strength and the elongation ϵ_{su} at maximum load was taken according to the classification (e.g. for class A steel: f_t=1,08·f_y, ϵ_{su}=5 %).

- Concrete C 35. The assumed peak stress in the stress-strain diagram was taken as f_{ck}. No confining reinforcement was assumed.

- Bond behavior approximately according to MC 90, Section 3.1.1, for bad bond conditions to model the situation over the support.

- The influence of shear cracks has been taken into account for shear forces higher than the value causing inclined shear cracks.

- The beam was loaded by a steel plate with a width of 150 mm. This means it has been assumed that the continuous slab is supported by e.g. a masonry wall.

- Failure has been assumed, if the peak moment has been obtained, i.e. either the steel reached the tensile strength at a strain ϵ=ϵ_{su} or the compression zone reached its bearing capacity. Therefore the increase of the plastic rotation in the descending branch of the moment-deflection diagram (compare Fig. 1) has been neglected. However, often the slab is supported by a rigidly connected concrete beam. The corresponding decrease of the rotation capacity has also not been taken into account (compare Fig. 23). These two effects may counterbalance each other.

The plastic rotation capacity calculated as explained above may represent the 5%-fractile of the values expected in tests with the corresponding type of steel. However, a certain margin of safety may be present in the assumptions.

In Fig. 24 the values x/d have been calculated in the conventional way using design values for the material properties, a parabolic-rectangular stress-strain diagram for the concrete with ϵ_{cu}=3,5 ‰ and a bi-linear stress-strain relationship for steel with ϵ_{su}=10 ‰.

Fig. 24 shows that the plastic rotation capacity given in MC 78 agrees approximately with the value valid for type S steel. For high values of x/d, failure will occur before yielding of the reinforcement. Therefore the influence of the type of reinforcement on the plastic rotation decreases with increasing value x/d. For values of the slenderness $l^*/d \neq 6$ the given plastic rotation capacity may be multiplied by the factor $((l^*/d)/6)^{0,5}$ (compare Fig. 22). l^* is the length of the zone between the points of zero moment (see Fig. 15).

In order to evaluate the possible degree of moment redistribution, the required plastic rotation must be known. It was calculated for continuous beams (rectangular section, tension reinforcement with f_{yk}=500 N/mm², no compression reinforcement) with a large number of equal spans under uniformly distributed load. The results are plotted in Fig. 25.

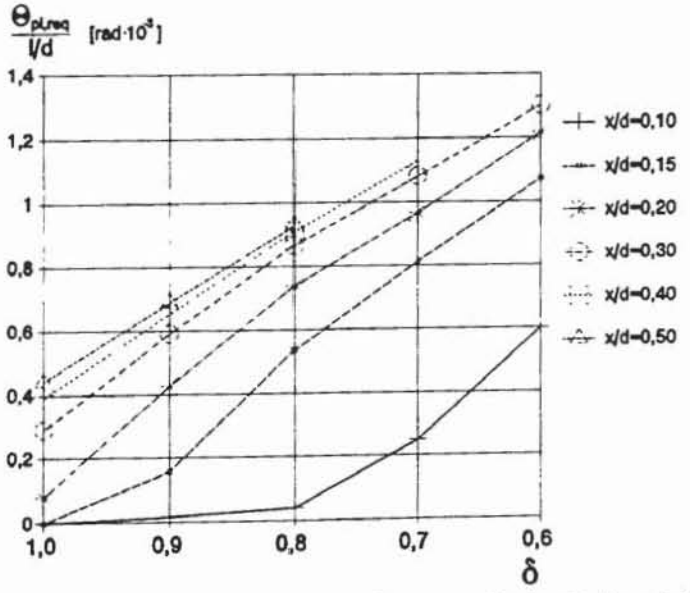

Figure 25: Required plastic rotation related to the slenderness l/d plotted over the degree of moment redistribution δ for a continuous girder under an uniformly distributed load

The assumed moment distributions are valid for different degrees of moment redistribution ($0,6 \leq \delta \leq 1,0$). The effect of tension stiffening on the moment-curvature relationship was assumed approximately according to MC 90, Section 3.2.3. The required plastic rotation is linear proportional to the slenderness l/d. Therefore in Fig. 25 $\Theta_{pl,req}$ is related to the slenderness l/d. One can see that the required plastic rotation increases almost linearly with increasing moment redistribution. For a value x/d=0,1 and $\delta \geq 0,8$ almost no plastic rotation is required, because the beam is practically uncracked.

The required plastic rotation shown in Fig. 25 compares favourably with the results presented by Cosenza et al. (1989).

Fig. 26 shows the influence of the concrete strength and of the steel yield strength on the required plastic rotation. The assumed statical system was a continuous girder under uniformly distributed load with a slenderness l/d=20 and with a moment redistribution of 20 %.

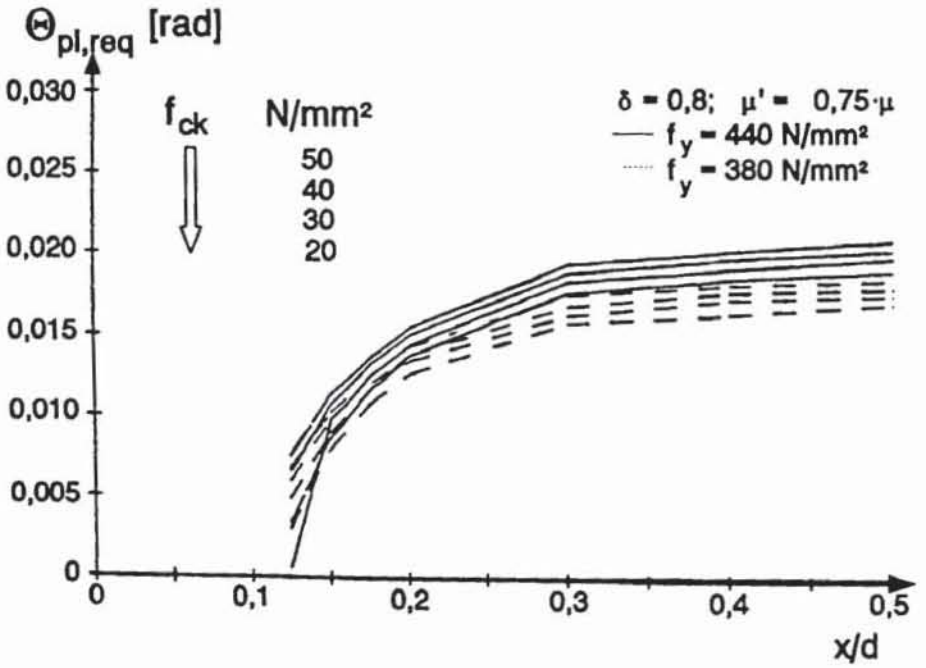

Figure 26: Influence of the concrete strength and of the steel yield strength on the required plastic rotation (δ=0,8 and l/d=20) (after Cosenza et al. (1989))

While the influence of the compression strength is rather small, the influence of the steel yield strength is more pronounced.

In Fig. 27a the available plastic rotation is compared with the required value for different degrees of moment redistribution ($0,6 \leq \delta \leq 1,0$). When calculating the required plastic rotation, it has been taken into account that for a given span of the cut out beam ($l^*/d=6$) the slenderness l/d of the continuous girder increases with increasing degree of moment redistribution from $l/d \approx 14$ ($\delta=1,0$) to $l/d \approx 27$ ($\delta=0,6$).

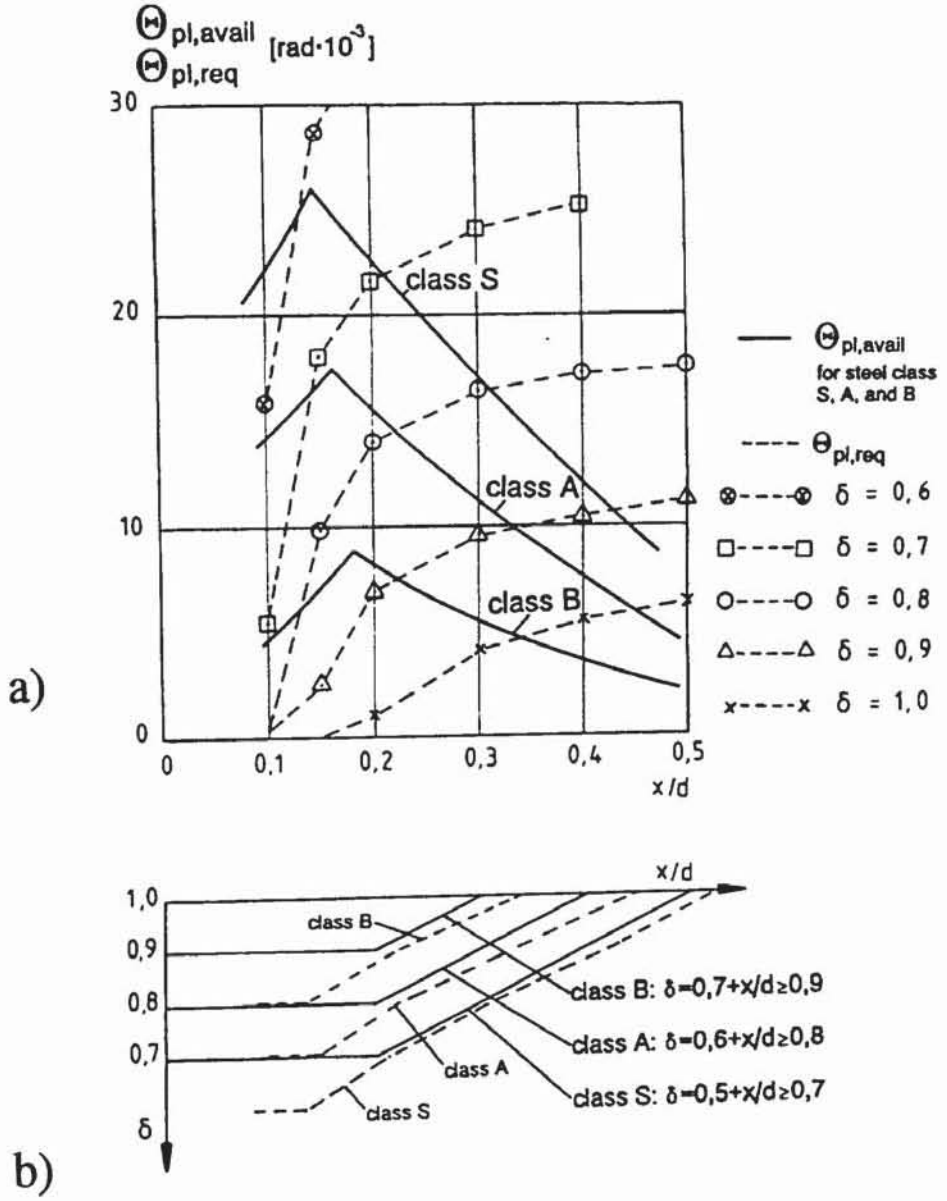

Figure 27: a) Comparison of available and required plastic rotation capacity
b) Proposal for the allowable degree of moment redistribution

The intersection of the curves representing the available and required plastic rotation, respectively, gives the maximum degree of moment redistribution. It is plotted in Fig. 27b as dotted lines.
It can be seen that the value for the allowable degree of moment redistribution depends significantly on the type of steel. The "real" behavior has been approximated by the full lines, which can be described by the following equations:

$$\text{Steel type B:} \quad \delta = 0{,}7 + x/d \geq 0{,}9 \tag{2a}$$

$$\text{Steel type A:} \quad \delta = 0{,}6 + x/d \geq 0{,}8 \tag{2b}$$

$$\text{Steel type S:} \quad \delta = 0{,}5 + x/d \geq 0{,}7 \tag{2c}$$

In equations (2) the maximum degree of moment redistribution has been limited to a smaller value than theoretically possible to take into account other loading cases and the current design experience.

The maximum degree of moment redistribution proposed above differs from the values proposed in MC 90 (compare Fig. 27b with Fig. 10 and eqn. (2) with eqn. (1)). The reason for this is that eqns. (1a) and (1b) were taken from MC 78 without considering the new diagram for the available plastic rotation capacity (see Fig. 5.4.2 of MC 90) and new studies by Cosenza et al (1989) on the influence of the concrete strength on the required plastic rotation (compare Fig. 26).

The required plastic rotation increases linearly with the slenderness l/d, while the available plastic rotation increases with $(l/d)^{0.5}$ only. Therefore, for larger or smaller values of the slenderness l/d than assumed above the maximum degree of redistribution is smaller or larger, respectively, than given by eqn. (2).

4 Summary

In this paper the provisions in MC 90 for the structural analysis and for the required ductility of steel are explained and

background material is given. In general, the provisions agree well with the current state of research. Some possible improvements are pointed out.

The ductility of the currently produced reinforcement differs considerably depending on the production method. Therefore three different steel classes in respect to ductility have been introduced in MC 90. This is correct from the scientific point of view but may cause serious problems on site (exchange of steel types). Therefore the ductility of steel type B should be improved to an acceptable degree so that for all non-seismic applications only one ductility class is required.

5 References

Bachmann, H. (1967): Zur plastizitätstheoretischen Berechnung statisch unbestimmter Stahlbetonbalken; Dissertation, ETH Zürich, 1967

Bachmann, H.; Thürliman, B. (1965): Versuche über das plastische Verhalten von zweifeldrigen Stahlbetonbalken, Serie A; Bericht Nr. 6203-1, Institut für Baustatik, ETH Zürich, Juli 1965

CEB-Fip-Model-Code 1978 (MC 78)

CEB-Fip-Model-Code 1990 (MC 90)

Ciampi, V.; Eligehausen, R.; Bertero, V. V.; Popov, E. P. (1982): Analytical model for deformed bar bond under generalized excitations; Report No. UCB/EERC-82/23, Earthquake Engineering Research Center, University of California, Barkley,1982

Cosenza, E.; Greco, C.; Pecce, M. (1989): Some remarks on the moment redistribution and on the evaluation of the required plastic rotations in r.c. continuous beams; Instituto di Tecnica delle Construzioni, Facolta' di Ingegneria, Napoli, Feb. 1989

Dilger, W. (1966): Veränderlichkeit der Biege- und Schubtragfähigkeit bei Stahlbetontragwerken und ihr Einfluß auf Schnittkraftverteilung und Traglast bei statisch unbestimmter Lagerung; Heft 179 der Schriftenreihe des DAfStb, Berlin, 1966

Eibl, J. (1991): Safty considerations for nonlinear analysis; IABSE Colloquium, Stuttgart, 1991

Eifler, H.; Plauk, G. (1974): Drehfähigkeit plastischer Gelenke in biegebeanspruchten Stahlbetonkonstruktionen; Bericht der Bundesanstalt für Materialprüfung (BAM) zum Forschungvorhaben BAM: Vh 221.2.221, Berlin, 1974, not published

Eligehausen, H.; Langer, P., Kreller, H. (1984): Anwendungstechnische Untersuchungen an Betonstahl; Bericht zum EGKS Forschungsvorhaben, Teil 1B, Verein Deutscher Eisenhüttenleute, Düsseldorf, 1984

Eligehausen, R.; Popov, E. P.; Bertero, V. V.: (1983): Local bond stress-slip relationship of deformed bars under generalized excitations; Report No. UCB/EERC 83/23, Earthquake Engineering Research Center, University of California, Berkley, 1983

Kreller, H. (1989): Zum nichtlinearen Trag- und Verformungsverhalten von Stahlbetontragwerken unter Last- und Zwangseinwirkung; Dissertation, Universität Stuttgart, 1989

Langer, P. (1987): Verdrehfähigkeit plastizierter Tragwerksbereiche im Stahlbetonbau; Dissertation, Universität Stuttgart, 1987

Macchi, G. (1979): Nonlinear analysis and design in the CEB Model Code; CSCE-ASCE-ACI-CEB International Symposium, University of Waterloo, Ontario, Canada, August 1979

Macchi, G. (1976): Ductility conditions for simplyfied design without check of compatibility, CEB-Bulletin No. 105, 1976

Martin, H.; Schießl, P.; Schwarzkopf, M. (1980): Ableitung eines allgemeingültigen Berechnungsverfahrens für Rißbreiten aus Lastbeanspruchung auf der Grundlage von theoretischen Erkenntnissen und Versuchsergebnissen; Heft 309 der Schriftenreihe "Straßenbau und Straßenverkehrstechnik", Bundesanstalt für Straßenwesen, Köln, 1980

Michalka, C. (1986): Zur Rotationsfähigkeit von plastischen Gelenken in Stahlbetonträgern mit Schubbewehrung; Dissertation, Universtät Stuttgart, 1986

Rao, P. S.; Kauman, P. R.; Subrahmanyam, B. V. (1971): Influence of span length and application of load on the rotation capacity of plastic hinges; Journal of the American Concrete Institut, June 1971

Schlaich, J.; Schäfer, K. (1989): Konstruieren im Stahlbetonbau, Betonkalender 1989, Verlag W. Ernst & Sohn, Berlin, 1989

Schlaich, J.; Schäfer, K.; Woidelko, E. O. (1982): Verhalten von Plattenbalken im Gebrauchs- und Bruchzustand, die nach Traglastverfahren bemessen worden sind; Institut für Massivbau, Universität Stuttgart, 1982, not published

Siviero, E. (1976): Rotation capacity of monodimensional members in structural concrete; CEB Bulletin No. 105, 1976

Steidle, P.; Schäfer, K. (1986): Trag- und Verformungsfähigkeit von Stützen bei großen Zwangsverschiebungen der Decken; Heft 396 der Schriftenreihe des DAfStb, Verlag W. Ernst & Sohn, Berlin, 1986